

Repairing of Anodic Oxide Films on Al - Zn Alloy Coated Steel after Removal with Photon Rupture in Solutions

Sakairi Masatoshi, Itabashi Kazuma, and Takahashi Hideaki

Graduate School of Engineering, Hokkaido University
Kita 13, Nishi 8, Kita-ku, Sapporo, 060-8628, Japan

Analysis of abrupt destroyed of passive oxide films on Al - Zn alloy layer coated on steel and its repair is important to understand the localized corrosion of steels. In the present investigation, anodic oxide films formed on Al - Zn coated steel specimens were removed by photon rupture method (one pulse of focused pulsed Nd - YAG laser beam irradiation) at a constant potential in sodium borate solutions, pH = 9.2, with / without chloride ions to monitor the current transient. Irradiation with a pulsed laser in solutions causes abrupt removal of the anodic oxide film on the specimen at the laser-irradiated area. Without chloride ions, oxide films were reformed in the sodium borate solution at - 0.5 to 1 V after removal of the anodic oxide film. However, in chloride ions containing solutions, pitting corrosion of Zn - 55 mass % Al coated layers occurs at high potentials, while film reformation occurs at low potentials. It was also found that chloride ions enhance dissolution of aluminum and zinc at the very initial period after laser irradiation.

Keywords : zinc - aluminum alloy coating, localized corrosion, photon rupture method, anodic oxide film, current transient

1. Introduction

Zn and Zn alloy coatings are widely used because of their excellent performance in corrosion protection of steels, particularly in atmospheric environments. The corrosion protection of steel by Zn and Zn alloy coatings is ascribed to cathodic protection by galvanic reaction between coated layer and substrate,¹⁾ and its high corrosion resistance due to the formation of stable and compact corrosion products.²⁻⁴⁾ Atmospheric corrosion studies have investigated the composition of corrosion products formed on Zn for various exposure conditions.⁵⁻⁹⁾ R. Ramanaukas et. al. has characterized corrosion products formed on electrodeposited Zn and Zn alloy in atmospheric environments such as marine and urban by x-ray diffraction and x-ray photoelectron spectroscopy.¹⁰⁾

For the application of electrochemical methods such as voltammetry, electrochemical impedance spectroscopy (EIS) to atmospheric corrosion study, some problems caused by thin electrolyte layer are encountered. Recently, the EIS technique has been applied to measurement of atmospheric corrosion of Zn or Zn alloy.¹¹⁻¹⁴⁾ Katayama et. al. has attempted to monitor the corrosion rate of Zn and Zn-Al coated steels under cyclic wet - dry conditions.¹¹⁾ The ex situ EIS studies of the initial stage of atmospheric zinc corrosion has reported by S. C. Chung

et. al.¹³⁾

Analysis of abrupt destroyed of passive oxide films on Al-Zn alloy layer coated on steel and its repair is important to understand the localized corrosion of steel. Analysis of this behavior has been carried out by monitoring potential- or current- transients after mechanically stripping¹⁵⁻²⁰⁾ of the oxide films. The mechanical film stripping poses problem in film stripping rate, contamination from stripping tools, and stress or strain on the substrate. Recently, film stripping by laser irradiation (photon rupture method), which resolves many of the problems has been reported. The irradiation of a pulsed laser beam is able to strip the oxide film at extremely high rate without any contamination of specimens. It has been used on iron electrodes by Oltra et al.,²¹⁻²⁵⁾ and on aluminum electrodes by Sakairi et al.^{25),26)} and Takahashi et al..²⁷⁾ Without chloride ions, oxide films were reformed in the borate solution after removal of the anodic oxide film by photon rupture method.^{25),26)} However, in chloride ion containing solutions, pitting corrosion occurs at high potentials, while film reformation occurs at low potentials. It was also found that chloride ions enhance dissolution of aluminum at the very initial period after laser irradiation.²⁷⁾

In the present investigations, zinc - aluminum alloy coated steel specimens covered with protective oxide film were irradiated with one pulse of pulsed Nd-YAG laser

beam at constant potential in sodium tetra-borate solutions with and without chloride ions to measure current transients.

2. Experimental

2.1 Specimen

Zn - 55 mass % Al coated steel sheet was cut into 20 x 20 mm with handle, and edges were covered by silicone. The coated layer thickness was about 19 μm . Specimens were anodizing in 0.1 kmol / m³ Na₂B₄O₇ (pH = 9.2), 0.1 kmol / m³ H₃BO₃ / 0.05 kmol / m³ Na₂B₄O₇ (pH= 8.7), and 0.5 kmol / m³ H₃BO₃ / 0.1 kmol / m³ Na₂B₄O₇ (pH = 7.4) solutions at 293 K with constant current density of 10 A / m², and then immersed for 120 s in boiling distilled water to seal the defects inside the film. After anodizing, film thickness and micro-structure were determined from observation of ultra-microtomed sections by transmission electron microscope (TEM).

2.2 Laser irradiation

The schematic model of laser irradiation system with current transient measurement unit shows in Fig. 1. The specimens were immersed in 0.1 kmol / m³ Na₂B₄O₇ and 0.1 kmol / m³ Na₂B₄O₇ with between 0.01 and 0.001 kmol / m³ NaCl solutions, and were irradiated with one pulse of the Nd-YAG laser beam focused on the surface with lens at constant potential, $E_s = -0.5$ to 1.0 V (vs. Ag / AgCl). The laser beam used was the second harmonic

wave with 532 nm wavelength, 8 ns puls duration, and laser power, P, was adjusted at 30 mW.

Current transients after laser irradiation were measured with a computer system through an A/D converter. The laser irradiation time was detected by photo-detector. After experiments, specimens surface were examined by confocal scanning laser microscope (CSLM).

3. Results and discussion

3.1 Anodizing of Zn-Al alloy layer

Fig. 2 shows potential time responses for Zn - 55 mass % Al coated steel at 10 A / m² in 0.1 kmol / m³ Na₂B₄O₇ (pH = 9.2), 0.1 kmol / m³ H₃BO₃ / 0.05 kmol / m³ Na₂B₄O₇ (pH= 8.7), and 0.5 kmol / m³ H₃BO₃ / 0.1 kmol / m³ Na₂B₄O₇ (pH = 7.4) solutions. In fig. 2, potential time curve for electropolished pure aluminum at 10 A / m² in 0.5 kmol / m³ H₃BO₃ / 0.1 kmol / m³ Na₂B₄O₇ (pH = 7.4) is also indicated as a solid line. The specimens show almost linear increase in potential with time. The slopes of potential time curves in high pH solutions are much steeper than that in low pH solutions, because of the dissolution rate of zinc is higher at lower pH solution.

Fig. 3 shows the TEM image of cross section of Zn - 55 mass % Al coated steel anodized at 10 A / m² in 0.1 kmol / m³ Na₂B₄O₇ (pH = 9.2) up to 50 V. The anodic oxide film formed on alloy coated layer has uniform thickness of about 70 nm. Thus the apparent film width / voltage ratio is about 1.4 nm / V. This value is about

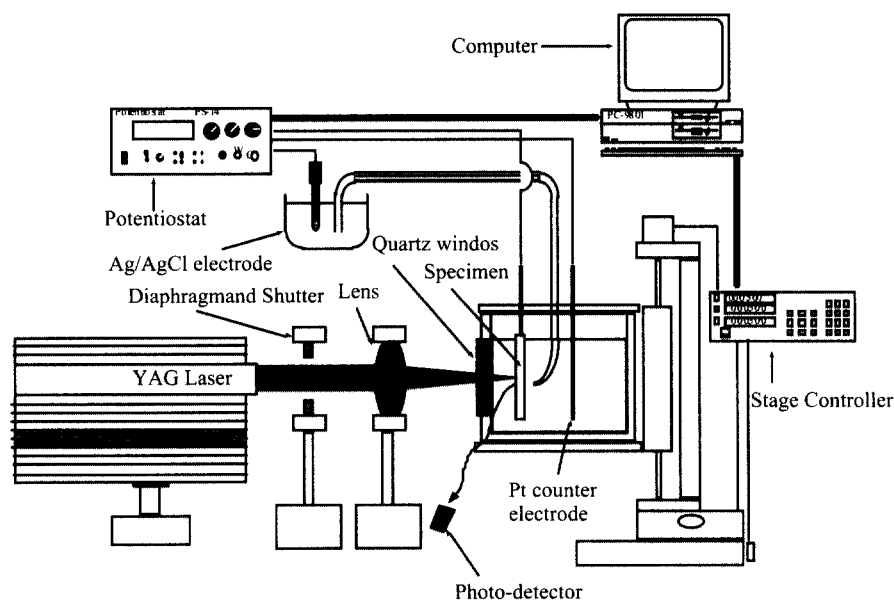


Fig. 1. Schematic diagram of laser irradiation system with electrochemical current measurement unit.

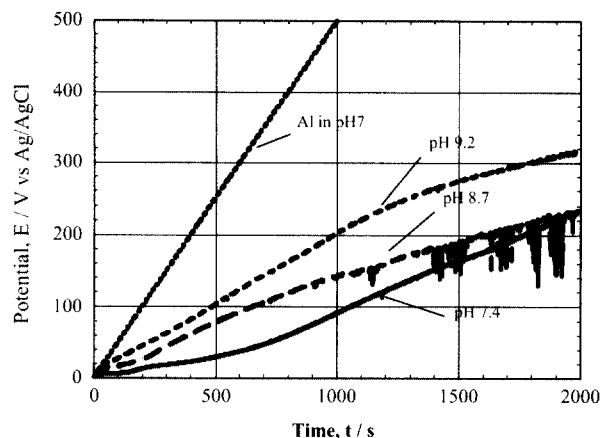


Fig. 2. Potential time response for Al and Zn - 55 mass % Al coated steel at 10 A / m^2 in $0.1 \text{ kmol / m}^3 \text{ Na}_2\text{B}_4\text{O}_7$ (pH = 9.2), $0.1 \text{ kmol / m}^3 \text{ H}_3\text{BO}_3 / 0.05 \text{ kmol / m}^3 \text{ Na}_2\text{B}_4\text{O}_7$ (pH = 8.7), and $0.5 \text{ kmol / m}^3 \text{ H}_3\text{BO}_3 / 0.05 \text{ kmol / m}^3 \text{ Na}_2\text{B}_4\text{O}_7$ (pH = 7.4) solutions.



Fig. 3. TEM image of vertical section of Zn - 55 mass % Al coated steel anodized at 10 A / m^2 in $0.1 \text{ kmol / m}^3 \text{ Na}_2\text{B}_4\text{O}_7$ (pH = 9.2) up to 50 V.

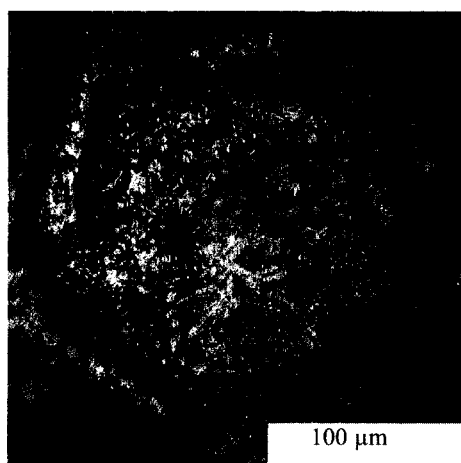


Fig. 4. CSLM surface image after laser irradiation at 1V in $0.1 \text{ kmol / m}^3 \text{ Na}_2\text{B}_4\text{O}_7$ solution.

30% larger than that of pure aluminum anodized at 10 A / m^2 in pH = 7.4 solution. The surface roughness increases during anodizing, because of zinc was dissolved. Surface color was changed bright to dark gray during sealing.

3.2 Film removal by photon rupture method

Fig. 4 shows the CSLM surface image after laser irradiation at 1V in $0.1 \text{ kmol / m}^3 \text{ Na}_2\text{B}_4\text{O}_7$ solution. The film removal area shows a pentagon, which comes from diaphragm, with about $200 \mu\text{m}$ diameter and rough surface, and it seems to have been quickly melted and solidified. It is considered that the anodic oxide film on Zn - 55 mass % Al alloy should be removed by the high pressure produced by laser ablation.

3.3 Current transient without chloride ions

The current transient and the photo detector signal between 0 to 10 ms after laser irradiation at $E_s = 1.0 \text{ V}$ in $0.1 \text{ kmol / m}^3 \text{ Na}_2\text{B}_4\text{O}_7$ solution is shown in Fig. 5. By laser irradiation, the current increases instantaneously and through a maximum, i_p , at about 0.4 ms after photo detector signal peak, decrease exponentially with time. About 600 ms after laser irradiation, the current reaches a value as low as that before laser irradiation.

Fig. 6 shows the change in current, i , with time, t , obtained in $0.1 \text{ kmol / m}^3 \text{ Na}_2\text{B}_4\text{O}_7$ solution at $E_s = -0.5$ and 1.0 V after laser irradiation. The slope of the $\log i$ vs. $\log t$ curves show about -0.3 at the initial stage, and then -1 at late stage after $t = 10 \text{ ms}$. The slope at the initial stage is slightly smaller as potential is set at higher values. At the initial stage after $t = 0.4 \text{ ms}$, the oxide film formation is accompanied by the film dissolution. The ratio of film dissolution rate to film formation rate increases as the set potential becomes nobler. At the late

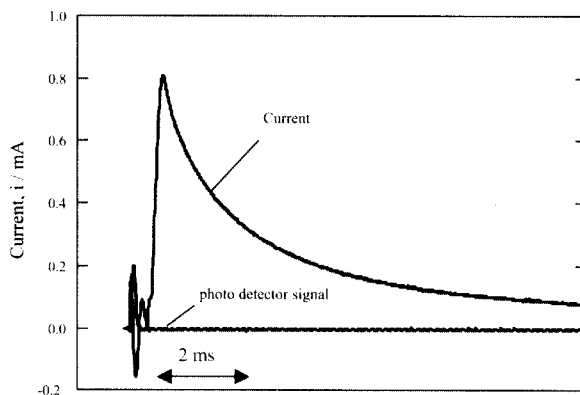


Fig. 5. Current transient and photo detector signal between 0 to 10 ms after laser irradiation at $E_s = -0.5$ in $0.1 \text{ kmol / m}^3 \text{ Na}_2\text{B}_4\text{O}_7$ solution.

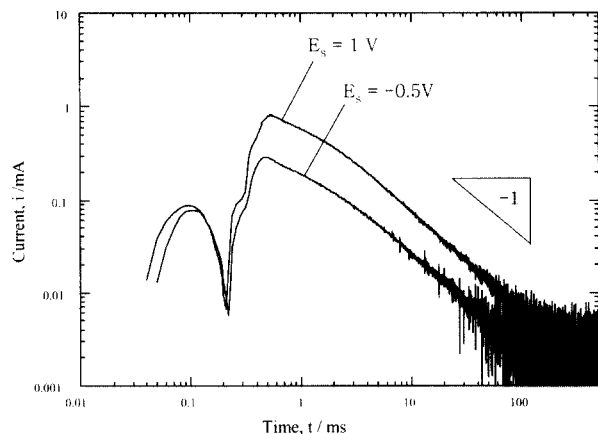


Fig. 6. Change in the current with time obtained in $0.1 \text{ kmol} / \text{m}^3 \text{ Na}_2\text{B}_4\text{O}_7$ solution at $E_s = -0.5$ and 1.0 V after laser irradiation.

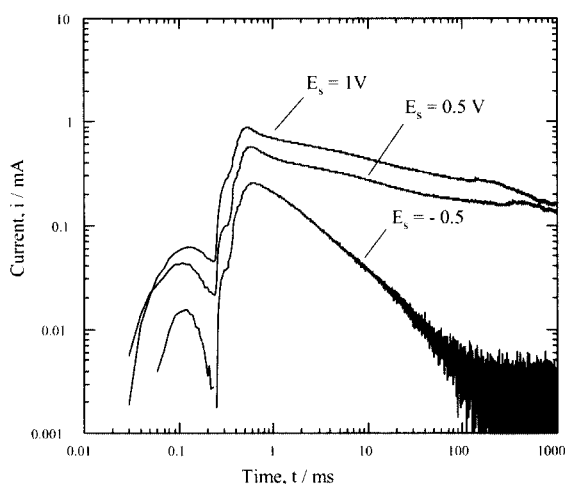


Fig. 7. Change in current with time obtained in $0.1 \text{ kmol} / \text{m}^3 \text{ Na}_2\text{B}_4\text{O}_7$ with $0.005 \text{ kmol} / \text{m}^3 \text{ NaCl}$ solution at $E_s = -0.5$, 0.5 and 1.0 V after laser irradiation.

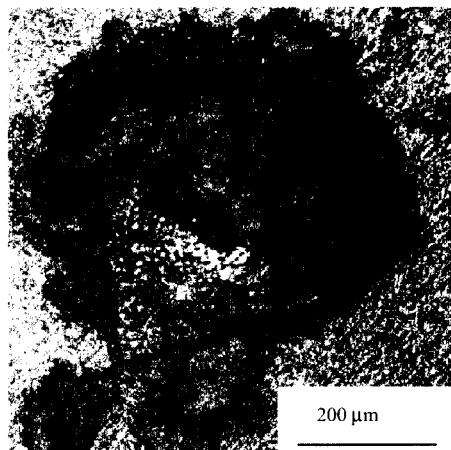


Fig. 8. CSLM image of specimen surface at $t = 5 \text{ s}$ after laser irradiation in $0.1 \text{ kmol} / \text{m}^3 \text{ Na}_2\text{B}_4\text{O}_7$ with $0.005 \text{ kmol} / \text{m}^3 \text{ NaCl}$ solution at $E_s = 1.0 \text{ V}$

stage after $t = 10 \text{ ms}$, the film formation kinetics follow the inverse logarithmic law, according to Cabrera-Mott theory.

3.4 Current transient with chloride ions

Fig. 7 shows the current transients obtained in $0.1 \text{ kmol} / \text{m}^3 \text{ Na}_2\text{B}_4\text{O}_7$ with $0.005 \text{ kmol} / \text{m}^3 \text{ NaCl}$ solution at $E_s = -0.5$, 0.5 and 1.0 V after laser irradiation. All the specimens show 0.4 ms of induction time before the abrupt increases and show the maximum of current, i_p , just after increasing. At $E_s = -0.5 \text{ V}$, current, i , decreases with time after the maximum and the slope of the $\log i$ vs. $\log t$ curves slightly smaller than one. Above $E_s = 0 \text{ V}$, i decreases with time and then increases after a minimum. As E_s becomes nobler, i increases. The behavior can be explained by a preferential dissolution of the metal substrate, which is enhanced at nobler potential.

Fig. 8 shows the CSLM image of specimen surface at $t = 5 \text{ s}$ after laser irradiation in $0.1 \text{ kmol} / \text{m}^3 \text{ Na}_2\text{B}_4\text{O}_7$ with $0.005 \text{ kmol} / \text{m}^3 \text{ NaCl}$ solution at $E_s = 1.0 \text{ V}$. White precipitates are observed at the laser irradiated area, which were produced by the preferential dissolution of the alloy layer. By electron probe micro analysis, these were considered to be aluminum hydroxides

3.5 Effect of chloride ion concentration on the preferential dissolution

Fig. 9 shows the effect of set potential, E_s , and chloride ion concentration on the peak current, i_p . The peak current, i_p , increases linearly with increasing set potential, E_s , in every solutions. At lower potential region, $E_s < 0 \text{ V}$, i_p independent of chloride ion concentration. However, at

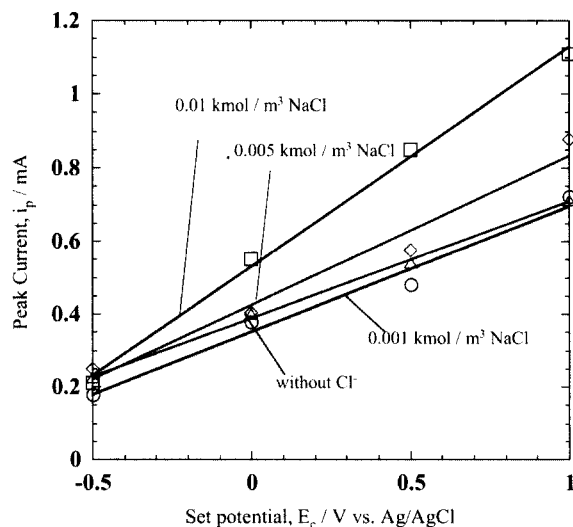


Fig. 9. Effect of the set potential, E_s , and chloride ion concentrations on the peak current, i_p .

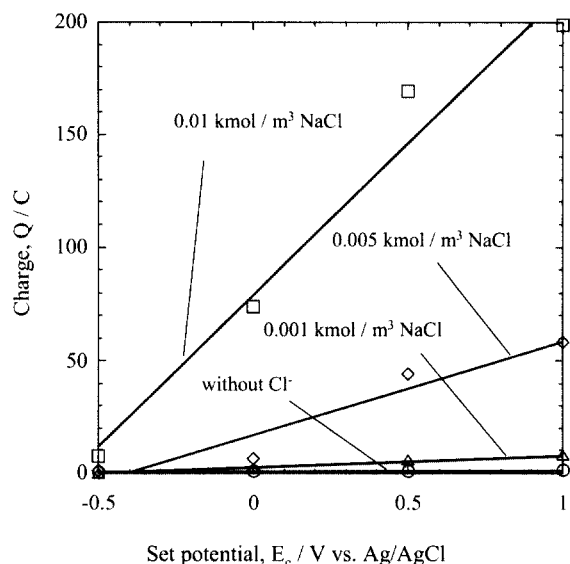


Fig. 10. Effect of the set potential, E_s , and chloride ion concentrations on the charge, Q .

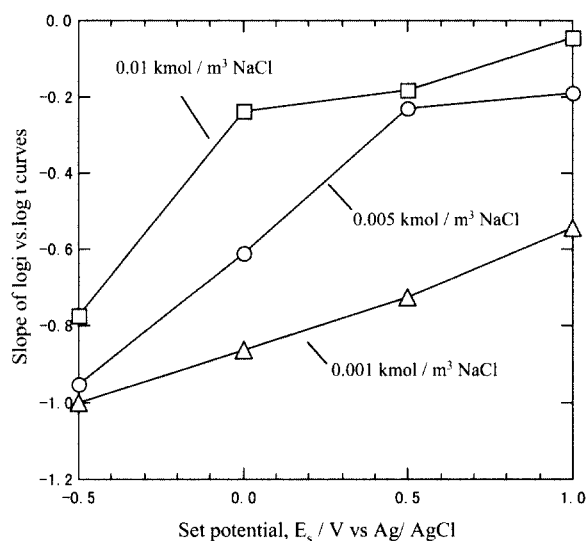
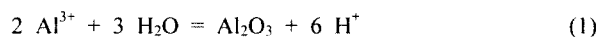


Fig. 11. Effect of set potential, E_s , and chloride ion concentrations on the slope of $\log t$ vs. $\log t$ curves.

higher set potential, $E_s > 0$ V, i_p increases with increasing chloride ion concentration. In without chloride ion solutions or at low set potentials, the Zn - 55 mass % Al layer exposed to the solution by the film removal is oxidized electrochemically to Zn^{2+} and Al^{3+} ions, and Al^{3+} ions react with water to form oxide film.



In the chloride ion containing solutions, the aluminum dissolution by forming aluminum-chloride complexes may

compete with Eq. 1 at high set potentials.



Zn^{3+} also dissolves as zinc-aquo complexes, Zn^{3+} (aq), after the layer is exposed to the solutions.

Fig. 10 shows the relationship between the charge, Q , and the set potential, E_s in $0.1 \text{ kmol} / \text{m}^3 \text{ Na}_2\text{B}_4\text{O}_7$ without and with 0.01, 0.005 and $0.001 \text{ kmol} / \text{m}^3 \text{ NaCl}$ solutions. The charge, Q , is independent of the set potential, E_s , in $\text{Na}_2\text{B}_4\text{O}_7$ without and with 0.01 and $0.005 \text{ kmol} / \text{m}^3 \text{ NaCl}$ solutions. However, in higher chloride ion concentrations, the charge, Q , increases linearly with increasing the set potential, E_s .

Fig. 11 shows the relationship between the slope $\log i$ vs $\log t$ plots after 10 ms and the set potential, E_s , in $0.1 \text{ kmol} / \text{m}^3 \text{ Na}_2\text{B}_4\text{O}_7$ with 0.01, 0.005 and $0.001 \text{ kmol} / \text{m}^3 \text{ NaCl}$ solutions. The slope become steeper at lower set potential and lower chloride ion concentration. This may be due to both aluminum and zinc dissolution, Eqs. 1 and 2 are enhanced by chloride ions and potential.

4. Conclusions

The photon rupture method was attempt to study initial stage of localized reformation of oxide film and localized corrosion on Zn - 55 mass% Al alloy coated steel specimens covered with protective oxide film, and the following conclusions may be drawn.

1) A dense anodic oxide film can be formed by anodizing of Zn - 55 mass % Al alloy coated steels in sodium borate solution at pH = 9.2. The anodic oxide film on the specimen can be removed locally by photon rupture method in solutions.

2) In sodium borate solution, oxide films are reformed between -0.5 to 1 V vs. Ag/AgCl after removal of the anodic oxide film.

3) Pitting corrosion occurs at high potentials, film reformation occurs at a low potentials in chloride ion containing solutions. The threshold potential for the pitting corrosion is higher at lower chloride ion concentration.

Acknowledgements

The authors wish to thank Dr. M. Kurosaki, Nippon Steel Co., for supply zinc and zinc - aluminum alloy coated samples. The work was financially supported by Grant - in- Aid for Encouragement of Young Scientists Japan Society for the Promotion of Science.

References

1. G. X. Zhang, "Corrosion and Electrochemistry of Zinc", Plenum Publication Co., New York (1996).
2. Y. Hisamatsu, *Bull. Jpn. Inst. Metals*, **20**, 3 (1981).
3. J. Oka, H. Asano, M. Takahsugi, and K. Yamamoto, *J. Iron and Steel Inst. Jpn.*, **68**, A57 (1982).
4. Y. Miyoshi, J. Oka, and S. Maeda, *Trans ISIJ*, **23**, 974 (1983).
5. T. E. Graedel, *J. Electrochem. Soc.*, **136**, 193C (1989).
6. J. E. Svensson and L. G. Johansson, *ibid.*, **143**, 51 (1989).
7. J. E. Svensson and L. G. Johansson, *Corrosion Sci.*, **34**, 721 (1993).
8. J. J. Frei, *Corrosion*, **42**, 422 (1986).
9. S. Oesch and M. Faller, *ibid.*, **39**, 1505 (1997).
10. R. Ramanauskas, P. Quintana, P. Bartolo-Perez, and L. Diaz-Ballote, *Corrosion*, **56**, 588 (2000).
11. H. Katayama Y. -C. Tay, A. S. Vioria, A. Nishikata, and T. Tsuru, *Mate. Trans. JIM.*, **38**, 1089 (1997).
12. G. A. EL-Mahdy, A. Nishikata, and T. Tsuru, *ibid.*, **42**, 183 (2000).
13. S. C. Chung, S. L. Sung, C. C. Hsine, and H. C. Shin, *J. Appl. Electrochem.*, **30**, 607 (2000).
14. C. Peiez, A. Collazo, M. Izquierdo, P. Merino, and X. R. Novoa, *Corrosion*, **56**, 1220 (2000).
15. F. P. Ford, G. T. Burstein, and T.P. Hoar, *J. Electrochem. Soc.*, **127**, 1325 (1980)
16. G. T. Burstein and P. I. Marshall, *Corros. Sci.*, **23**, 125 (1983).
17. G.T. Burstein and R. C. Newman, *Electrochim. Acta*, **25**, 1009 (1980).
18. G.T. Burstein and R. J. Cinderey, *Corros. Sci.*, **32**, 1195 (1991).
19. R. J. Cindery and G. T. Burnstein, *ibid.*, **33**, 493 (1992).
20. R. J. Cindery and G. T. Burnstein, *ibid.*, **33**, 499 (1992).
21. R. Oltra, G. M. Indrianjafy, and M. Keddama, *Materials Science Forum*, **44 & 45**, 259 (1989).
22. R. Oltra, G. M. Indrianjafy, and R. Roberge, *J. Electrochem. Soc.*, **140**, 343 (1993).
23. R. Oltra, G. M. Indrianjafy, M. Keddama, and H. Takenouti, *Corros. Sci.*, **35**, 827 (1993)
24. M. Itagaki, R. Oltra, B. Vuillemin, M. Keddama, and H. Takenouti, *J. Electrochem. Soc.*, **144**, 64 (1997).
25. M. Sakairi, Y. Ohira, and H. Takahashi, *Electrochem. Soc. Proc.*, **Vol. 97-26**, 643 (1997).
26. M. Sakairi, Y. Ohira and H. Takahashi, *Zairyo-Kagaku*, **34**, 275 (1997).
27. H. Takahashi, M. Sakairi, and Y. Ohira, *Electrochem. Soc. Proc.*, **Vol. 99-27**, 377 (1999).